Brain Stimulation 14 (2021) 316–326

Contents lists available at ScienceDirect

Brain Stimulation

journal homepage: http://www.journals.elsevier.com/brain-stimulation

The impact of individual electrical fields and anatomical factors on the neurophysiological outcomes of tDCS: A TMS-MEP and MRI study

Mohsen Mosayebi-Samani [a, b], Asif Jamil [a], Ricardo Salvador [c], Giulio Ruffini [c], Jens Haueisen [b], Michael A. Nitsche [a, d, *]

[a] Department Psychology and Neurosciences, Leibniz Research Centre for Working Environment and Human Factors, Dortmund, Germany
[b] Institute of Biomedical Engineering and Informatics, Technische Universität Ilmenau, Ilmenau, Germany
[c] Neuroelectrics, Cambridge, MA (US) and Barcelona, Spain
[d] Department of Neurology, University Hospital Bergmannsheil, Bochum, Germany

ARTICLE INFO

Article history:
Received 25 August 2020
Received in revised form
11 January 2021
Accepted 19 January 2021
Available online 28 January 2021

Keywords:
Inter-individual variability
Computational neurostimulation
tDCS
FEM
TMS
MEP
CBF
fMRI

ABSTRACT

Background: Transcranial direct current stimulation (tDCS), a neuromodulatory non-invasive brain stimulation technique, has shown promising results in basic and clinical studies. The known interindividual variability of the effects, however, limits the efficacy of the technique. Recently we reported neurophysiological effects of tDCS applied over the primary motor cortex at the group level, based on data from twenty-nine participants who received 15min of either sham, 0.5, 1.0, 1.5 or 2.0 mA anodal, or cathodal tDCS. The neurophysiological effects were evaluated via changes in: 1) transcranial magnetic stimulation (TMS)-induced motor evoked potentials (MEP), and 2) cerebral blood flow (CBF) measured by functional magnetic resonance imaging (MRI) via arterial spin labeling (ASL). At the group level, dose-dependent effects of the intervention were obtained, which however displayed interindividual variability.

Method: In the present study, we investigated the cause of the observed inter-individual variability. To this end, for each participant, a MRI-based realistic head model was designed to 1) calculate anatomical factors and 2) simulate the tDCS- and TMS-induced electrical fields (EFs). We first investigated at the regional level which individual anatomical factors explained the simulated EFs (magnitude and normal component). Then, we explored which specific anatomical and/or EF factors predicted the neurophysiological outcomes of tDCS.

Results: The results highlight a significant negative correlation between regional electrode-to-cortex distance (rECD) as well as regional CSF (rCSF) thickness, and the individual EF characteristics. In addition, while both rCSF thickness and rECD anticorrelated with tDCS-induced physiological changes, EFs positively correlated with the effects.

Conclusion: These results provide novel insights into the dependency of the neuromodulatory effects of tDCS on individual physical factors.

1. Introduction

Transcranial direct current stimulation (tDCS), as a non-invasive brain stimulation (NIBS) tool, changes regional cortical excitability in a polarity-dependent way, via delivering weak direct electrical currents, by electrodes placed on the head [1]. Despite promising results reported in pilot studies, effects are however largely moderate, show interindividual variability, and more sustained, and homogeneous effects are required, especially for clinical applications [2,3].

Heterogeneous results can be explained by inconsistency of the used stimulation parameters, and other methodological differences between studies, but also interindividual variability of tDCS outcomes [3,4]. The latter has been reported as one of the major challenges regarding tDCS applicability for basic research, and clinical purposes [5,6]. Various sources of variability have been identified, including physical (brain anatomy [7], tissue properties

* Corresponding author. Department Psychology and Neurosciences, Leibniz Research Centre for Working Environment and Human Factors, Dortmund, Germany.
E-mail address: nitsche@ifado.de (M.A. Nitsche).

https://doi.org/10.1016/j.brs.2021.01.016

[8,9] and neural orientation [10]), physiological (genetics [11], sex- and age-dependency [12,13], pharmacology [14]), and functional factors (psychological and behavioral processes [15,16]).

While causes of variability have yet to be explored in detail, recent human *in-vivo* experiments [17,18], and current-flow simulations indicate that both, spatial distribution and intensity of the tDCS-induced electrical field (EF) depend strongly on individual brain anatomy and tissue conductivity properties; biophysical factors that can potentially impact the outcome of tDCS. This highlights the importance of understanding and controlling these biophysical factors on neurophysiological and/or behavioral effects of tDCS at the individual level.

Up to now, a few studies highlighted the explanatory power of anatomical factors (e.g. thickness of cerebrospinal fluid (CSF)) to explain tDCS-induced EF variability across individuals [7,19]). In addition, a few pilot studies have shown an association between neurophysiological (e.g. tDCS-induced motor evoked potential (MEP) changes [20,21], tDCS-altered GABA concentration [22]), and behavioral effects of tDCS (e.g. tDCS-altered working memory performance [23]), and EF differences at the group level. Furthermore, this approach has been used to investigate the variability of other NIBS modes (e.g. transcranial alternating current stimulation-induced aftereffects on α-oscillations [24], or transcranial magnetic stimulation (TMS) effects and MEP amplitude changes). However, it is still unclear whether and to what degree these individual physical factors affect and/or explain the individual neurophysiological outcome of tDCS in detail. A systematic investigation of the impact of these factors on the neuroplastic effects of different tDCS dosages is therefore required.

In addition, the regional neuroplastic after-effects of tDCS have largely been investigated for the motor cortex with TMS. Neuroanatomical findings, as well as computational modeling studies, have highlighted the contribution of the sensorimotor network to TMS-elicited MEP [25–27]. This suggests that a computational model designed to investigate tDCS effects, based on motor cortex excitability measures, should also account for the EF distribution of TMS.

In two consecutive studies, we systematically titrated the effects of 15min of anodal and cathodal tDCS over the motor cortex at five intensities (sham, 0.5, 1.0, 1.5 and 2.0 mA), evaluated via (1) changes in TMS-induced MEP (tDCS-*TMS-MEP*) [28], and (2) changes in cerebral blood flow (CBF) measured by functional magnetic resonance imaging (fMRI) (tDCS-*fMRI*) [29], for up to 2 h after intervention. The results of the tDCS-*TMS-MEP* experiment show equivalent facilitatory after-effects at all tested anodal tDCS intensities, while for cathodal tDCS, only 1.0 mA resulted in a sustained significant corticospinal excitability reduction. The outcome of the tDCS-*fMRI* experiment, in which the same participants were involved, revealed an increased CBF under the M1 electrode after anodal tDCS with all intensities, while after cathodal stimulation decreased CBF was observed, with the exception of 0.5 mA in both stimulation polarity conditions.

In the present study, based on these data we explored whether and to which extent the neurophysiological outcome of tDCS, at the individual level, can be explained by considering individual anatomical, and resulting EF factors. For that, individual MR-based realistic head models were developed to simulate tDCS- and TMS-induced EF, and calculate also individual anatomical factors. We then investigated how much these individual anatomical factors explained simulated EF variability. In addition, we explored whether specific anatomical and/or EF factors explained the neurophysiological outcomes of tDCS (including MEP and CBF). Based on previous findings, we anticipated a that larger MEP and/or CBF changes would be linked with higher EF induction, while anatomical factors resulting in lower EF magnitudes would impact negatively on tDCS-induced neurophysiological alterations.

2. Materials and methods

2.1. Participants

The data of twenty-nine healthy, young and right-handed [30] participants (16 males, mean age 25.0 ± 4.44 years) who were involved in our former experiments [28,29] were selected. In these experiments, participants were randomly allotted to two groups of anodal (n = 15), or cathodal tDCS (n = 14). None of the participants had a history of neurological or psychiatric disease, and none fulfilled exclusion criteria for tDCS, TMS, and MRI [31,32]. Central nervous system-acting medication or respective recreational substances served also as exclusion criteria. Subjects were instructed not to consume caffeine, alcohol, or engage in strenuous physical activities 24 h prior to each session to ensure a stable level of motor-cortical excitability. The study conformed to the Declaration of Helsinki and was approved by the Medical Ethics Committee of the University of Göttingen.

2.2. tDCS over the primary motor cortex

For both experiments, tDCS was applied with an MR-compatible battery-powered constant current stimulator (neuroCare, Ilmenau, Germany), through a pair of surface rubber electrodes placed on the scalp (covered with a saline soaked sponge for the 'tDCS-*TMS-MEP*' experiment, and a layer of conductive paste (Ten20®, Weaver) for the 'tDCS-*fMRI*' experiment). The target electrode (35 cm^2) was fixed over the motor cortex representational area of the right abductor digiti minimi muscle (ADM) as identified by TMS ('ADM hotspot'), and the return electrode (100 cm^2) was placed contralaterally over the right orbit. A topical anesthetic cream (EMLA®, AstraZeneca, UK) was applied to the stimulation site, to reduce stimulation discomfort and improve blinding [33]. Based on the experimental group and session conditions, anodal or cathodal tDCS at an intensity of 0.5, 1.0, 1.5, 2.0 mA, or sham was delivered for 15 min, with a 10 s ramp at the beginning and end of stimulation. For sham, 1.0 mA stimulation was delivered for 30 s, with a 20sec ramp, followed by 15 min with 0.0 mA stimulation.

2.3. Motor cortical excitability assessment by TMS-induced MEPs

Monophasic TMS pulses were delivered by a Magstim 200 magnetic stimulator (Magstim, Whiteland, UK) through a figure-of-eight-shaped coil (diameter of one winding 70 mm; peak magnetic field 2 T) at a frequency of 0.25 Hz with 10% jitter. The coil was held tangentially to the scalp at an angle of 45° to the sagittal plane with the handle pointing laterally and posterior. MEP signals were sampled (5 kHz), amplified and bandpass filtered at 2 Hz–2kHz (Digitimer, Welwyn Garden City, UK), and recorded/controlled with Signal software v.2.13 (CambridgeElectronicDesign, Cambridge, UK).

2.4. Structural and functional MRI acquisition

For the 'tDCS-*fMRI*' experiment, MR scans were conducted in a 3 T Magnetom TrioTim (SiemensHealthcare, Erlangen, Germany) using a 32-channel head coil. Before subjects were placed inside the magnet bore, stimulation electrodes were fitted over the targeted area (as explained in section 2.2). First, anatomical T1-weighted MRI at 1 mm^3 resolution was recorded. Then three measurements of 1) resting-state blood-oxygen-level-dependent (BOLD), 2) resting-state arterial spin labeling (ASL), and 3) gradient echo field

mapping scans, were obtained before stimulation (baseline), during, and immediately as well as 15, 30, 45, 60, 75, 90, 105, and 120min after stimulation. For details of the MR image acquisition, see supplementary materials.

2.5. tDCS-induced electrical field simulation

Each participant's T1 image was first automatically segmented into seven head tissue compartments, including white matter (WM), gray matter (GM), CSF, skull, scalp, eyeballs and air cavities, using the SPM12 software package including an improved tissue probability map [34]. A custom MATLAB (R2019a, MathWorks, MA)script was then used to correct for automatic segmentation errors [34]. Afterwards, a 3D head model, based on the segmented images, was developed using Simpleware ® software (Synopsys, Inc., Mountain View, USA), with electrodes (2 mm thickness) and Ten20 paste (3 mm thickness) precisely located on the head over the targeted areas determined by visual inspection of the structural T1 images, using the render view of MRIcron, and a custom Matlab script for electrode placement [34]. The 3D head model was then meshed with tetrahedral elements using adaptive meshing (+ScanFE, Simpleware software). The volume-meshed model was imported to the COMSOL Multiphysics software package v.5.5 (COMSOL Inc., MA, USA), and tissue electrical conductivity values were assigned (in S/m): GM : 0.276; WM : 0.126; CSF : 1.65; skull : 0.01; scalp : 0.465; air : 2.5×10^{-14} Ten20 paste : 1.5; electrode rubber : 29 [18,35,36].The EF was then calculated under the quasi-static approximation for 1 mA tDCS [37]. Finally, the EF magnitude, $|E| = \sqrt{{E_x}^2 + {E_y}^2 + {E_z}^2}$, and the component of the EF perpendicular to the interface, $nE = \vec{n}_x.\vec{E}_x + \vec{n}_y.\vec{E}_y + \vec{n}_z.\vec{E}_z$ (where $\vec{n}$ is the inner normal vector to the cortical surface), on the mesh grids, which were imported to MATLAB, and interpolated then onto a regular grid similar to the original MR images (1 mm^3), Fig. 1C.

2.6. TMS-induced electrical field simulation

First, a realistic model of the coil (Magstim 70 mm figure-of-eight) was designed using AutoCAD (Autodesk Inc., CA, USA), with two circular wings with nine turns each and a wire cross section of 1.75 mm × 6 mm [38], and imported to Simpleware® software (+ScanCAD). The coil was then precisely placed over the individual head model, with the center placed at the midpoint of the tDCS target electrode and 3 mm distance to the scalp, and the handle held 45° to the midline. The head and coil models were then placed inside a spherical surrounding composed of air, and the full model was meshed with tetrahedral elements using an adaptive meshing algorithm (+ScanFE, Simpleware®). The volume-meshed model was finally imported to COMSOL Multiphysics software package to calculate the total EF ($\vec{E} = -\frac{d\vec{A}}{dt} - \vec{\nabla}\phi$, where $\vec{A}$ and ϕ represent the magnetic vector potential and the electric scalar potential, respectively), for a monophasic pulse (current derivative $\frac{dI}{dt} = 67$ A/μs) delivered by the coil connected with the Magstim 200 stimulator to induce a posterior–anterior current flow in the brain, Fig. 1C. Electrical conductivity of the respective head tissue compartments was assigned as in the tDCS simulation, in addition with an electrical permittivity of 10^4 for all head tissues [39], coil (5.8×10^7S/m) [40], and surrounding air (permittivity of free space, and a conductivity of 2.5×10^{-14}S/m). The EF results were finally imported to MATLAB and interpolated onto a similar regular grid of the MR anatomical images (1 mm^3).

2.7. Experimental procedure: 'tDCS-TMS-MEP' and 'tDCS- fMRI'

The details of the experimental procedures can be found in our former studies [28,29]. Briefly, for the 'tDCS-*TMS-MEP*' experiment, subjects were seated in a comfortable chair with head and arm rests. First the ADM hotspot was identified, and TMS intensity adjusted to elicit MEPs with a peak-to-peak amplitude of on average 1 mV (SI_{1mV}). Afterwards, baseline cortical excitability was determined by measuring 25 MEPs, following 15min of anodal or cathodal stimulation (in five sessions: sham, 0.5, 1.0, 1.5, and 2.0 mA). After finishing the stimulation, cortico-spinal excitability was assessed by TMS measurements, every 5 min for up to 30min, and then 60min, 90min, 120min after tDCS (Fig. 1A. Experiment 1).

For the *'tDCS-fMRI'* sessions, stimulation electrodes were first placed over the head with the target electrode positioned over the 'ADM hotspot', as identified by TMS measures, and the return electrode over the right supraorbital region. Subjects were then situated comfortably inside the scanner, to obtain an initial T1 anatomical scan, followed by baseline measures: resting-state BOLD, ASL sequences, and a Field Mapping sequence in counterbalanced order. Then, anodal or cathodal tDCS was delivered for 15 min in five sessions in randomized order (as explained above); one resting-state block was recorded during stimulation. After finishing stimulation, the tDCS device was turned off, and the after measures resting-state blocks were acquired in intervals of 15 min until 120 min after the end of stimulation (Fig. 1B. Experiment 2). For both experiments, there was at least one-week interval between each session to avoid carry-over effects.

2.8. Calculations and statistical analysis

2.8.1. Neurophysiological effects of tDCS (TMS-MEP and ASL-fMRI)

Details of the calculations and statistical analyses of the MEP and CBF data are available in our former studies [28,29]. Briefly, for the 'tDCS-TMS-MEP' experiment, individual means of each time point's MEP amplitudes (MEP_t) were calculated and then normalized to baseline MEPs (MEP_{bl}): $nMEP = (MEP_t / MEP_{bl})$. For the 'tDCS-ASL-fMRI' experiment, the grand-average mean perfusion time course of the voxels was averaged over the time-series (CBF_t) and then normalized to the pre-stimulation baseline (CBF_{bl}): $nCBF = (CBF_t / CBF_{bl})$. Then, to compensate for variability between time-points, the after-stimulation MEP amplitudes (ten time-points), and CBF values (eight time-points; excluding the scanning block during stimulation) were separately grand-averaged and pooled into two epochs of early (0–60min after-stimulation) and late (75–120min after-stimulation) effects. Thereafter, square root transformation was applied to the pooled values, which has been shown to improve the normality of data distribution, required for the used statistical analysis [41]. The distribution of the data was then assessed with the Kolmogorov–Smirnov procedure, and no significant deviations from normality were detected (for details see supplementary materials Table 3).

2.8.2. Regions of Interest

We defined two ROIs: 1) ROI_{HK}, and 2) ROI_{TMS}. The ROI_{HK} was selected to explore the direct tDCS effects over the hand knob motor representation area, which was defined in the cortex using a 2.5 cm radius sphere centered at MNI coordinates (x = −37.4, y = −19.1, z = 52.4 mm [42]). The ROI_{TMS} was selected based on neuroanatomical and computational studies, suggesting the contribution of different neural generators of the sensorimotor network for the TMS-evoked MEP [25–27]. We first extracted the respective regions (Brodmann areas corresponding to the left sensorimotor network, including the somatosensory cortex (BA1, BA3), M1 (BA4), and the premotor cortex (BA6)) from the

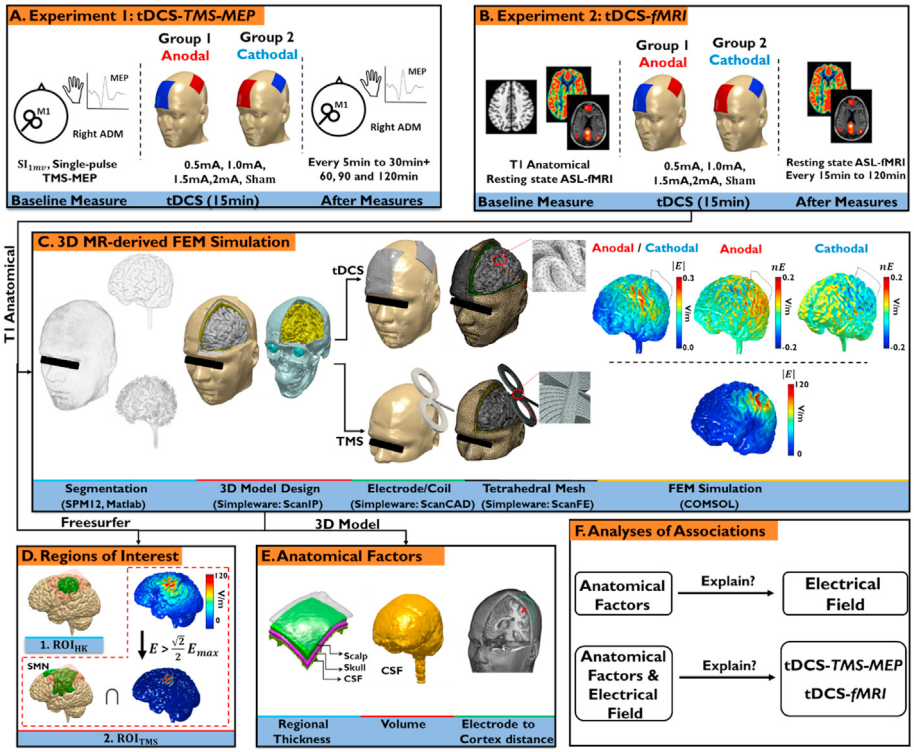

Fig. 1. Study design. Twenty-nine participants, who took part in two consecutive experiments, were randomly divided into two groups (Anodal: n = 15; Cathodal: n = 14). In each group, participants received 15min of sham, 0.5, 1.0, 1.5 or 2.0 mA motor tDCS. **A) *Experiment 1- 'tDCS-TMS-MEP'***: tDCS effects on corticospinal excitability were assessed by single-pulse TMS-MEP, for up to 2 h after intervention. **B) *Experiment 2- 'tDCS-fMRI'***: tDCS effects on cortical neurovascular activity were investigated using resting state ASL-fMRI, as a measure of CBF, for up to 2 h after tDCS. **C) *3D MR-derived FEM simulation***: the anatomical image was first automatically segmented into seven major head tissues using the SPM12 toolbox and a custom MATLAB script, and then imported to the Simpleware software package to: 1) design a 3D model of the head including tDCS electrodes, or TMS coil, and 2) mesh the model. The EF distribution was finally estimated using COMSOL software for 1 mA tDCS (magnitude (|*E*|) and normal component (*n*E)), and TMS (|*E*|). **D) *Regions of Interest* (ROI):** 1) ROI_{HK}: sphere (r = 2.5 mm) around motor hand knob and 2) ROI_{TMS} :intersection of sensorimotor network (SMN) and the cortical region in which the EF meet the predefined condition: $E > \frac{\sqrt{2}}{2} E_{max}$. **E) *Anatomical Factors:*** individual anatomical measures were conducted, including regional (under the target electrode) thickness of scalp, skull and CSF, and CSF volume, in addition to target electrode to cortex distance. **F) *Analyses of Associations*:** we explored if anatomical factors explain individual EF variability, and whether and to what extent the individual anatomical factors and/or EFs explain the variability of the neurophysiological outcomes of tDCS (MEP and CBF measures).

parcellated Brodmann atlas generated by Freesurfer reconstruction of each individual T1 image. We then defined an area over this region, where the TMS-induced EF met the predefined condition $E > \frac{\sqrt{2}}{2} E_{max}$; the half power region [43], Fig. 1D.

2.8.3. Anatomical measures

The regional thickness of scalp, skull, and CSF (rCSF) were measured for the individual head models by selecting the compartment corresponding to the target electrode (plus an additional 2 cm at each side to include the area in which the target electrode exerted strong effects [19]) and extruding the layer of the thickness dimension to include the tissue regions underneath. In addition, the whole CSF volume (without ventricles) was obtained for each individual head model by the Simpleware measurement tools. For the determination of regional electrode to cortex distance (rECD), first, the center of each electrode was identified by a rendered view of MRIcron, and the Euclidian distance was then calculated from this location to the individual hand motor area coordinate (MNI coordinates: x = −37.4, y = −19.1, z = 52.4 mm [42]), Fig. 1E.

2.8.4. Statistics

Multiple linear regressions were first applied to investigate if the individual averaged EF (|E| and *n*E) for the ROI_{HK} or ROI_{TMS} (as dependent variable) can be explained by respective individual anatomical factors (as explanatory variables). The same statistical analysis was then used to test whether and to which extent the individual variability of the neurophysiological effects of tDCS (including MEP and CBF as dependent variables) can be explained by the respective individual EFs, or anatomical factors. For CBF, we only used EF for the ROI_{HK} because of the missing TMS condition in the MRI experiment. In addition, for each regression analysis, we further calculated Pearson's correlation coefficient to identify the directionality of the predictors. Note that EFs were calculated for 1 mA tDCS. This was done because for the statistical analyses (linear regression/Pearson correlation), the relative EF between subjects is required, and this relation will be the same for all intensities. We thus chose one 1 mA for the calculations. It should be noted that the estimated EFs can be linearly scaled for other tDCS intensities based on the quasi-static approximation [37], and, therefore different absolute EFs magnitudes due to different stimulation intensities do not affect the statistical analyses and results (see supplementary Figure 4). The respective p-values were adjusted for multiple comparisons via the False Discovery Rate (FDR).

3. Results

The individual tDCS- and TMS-induced EF distributions are shown in supplementary materials Figs. 2 and 3 **tDCS-induced MEP and CBF alterations:** The detailed results of the neurophysiological effects of tDCS are available in our former studies [28,29]. Briefly, for the 'tDCS-TMS-MEP' experiment, significant facilitatory effects were observed for all anodal active tDCS protocols, while for

cathodal tDCS, only 1.0 mA resulted in a sustained excitability diminution. For the 'tDCS-fMRI' experiment, CBF increased under M1 for anodal tDCS with 1 mA and 2 mA intensity (most clearly in early epochs), while all active cathodal conditions (with the exception of 0.5 mA intensity) decreased CBF (most clearly in the late epochs) (supplementary material, Fig. 1). **Association between Anatomical Factors and Electrical Fields:** the results indicate that for both, the anodal and cathodal groups, both rCSF thickness and rECD significantly anticorrelated with the |E| and nE at ROI_{HK} and ROI_{TMS} (with the exception of rECD for nE at ROI_{TMS}). The remaining anatomical factors had no significant predictive value (Fig. 2; see supplementary materials for the calculated anatomical factors, and EF values (Table 1), and the resulting statistical analyses (Table 5), Fig. 5).

3.1. Association between anatomical factors, electrical fields and tDCS-induced MEP alterations

The statistical results indicated that, for the *anodal group* at the early epoch, rCSF thickness significantly predicted the MEP variabilities of stimulation intensities (0.5 mA-tDCS: $R^2 = 0.42$, $p_{FDR} = 0.027$, r = −0.65, 1.0 mA-tDCS: $R^2 = 0.45$, $p_{FDR} = 0.015$, r = −0.67 and 2.0 mA-tDCS: $R^2 = 0.41$, $p_{FDR} = 0.033$, r = −0.64), and also rECD had significant predictive power (0.5 mA-tDCS: $R^2 = 0.37$, $p_{FDR} = 0.046$, r = −0.58, and 1.5 mA-tDCS: $R^2 = 0.58$, $p_{FDR} = 0.004$, r = −0.76). In addition, |E| predicted MEP variance significantly (ROI_{HK}: 0.5 mA-tDCS: $R^2 = 0.42$, $p_{FDR} = 0.027$, r = 0.65, 1.0 mA-tDCS: $R^2 = 0.45$, $p_{FDR} = 0.015$, r = 0.67, and 1.5 mA-tDCS: $R^2 = 0.57$, $p_{FDR} = 0.005$, r = 0.76; ROI_{TMS}: 0.5 mA-tDCS: $R^2 = 0.41$, $p_{FDR} = 0.025$, r = 0.64, 1.0 mA-tDCS: $R^2 = 0.60$, $p_{FDR} = 0.009$, r = 0.78, 2.0 mA-tDCS: $R^2 = 0.38$, $p_{FDR} = 0.042$, r = 0.61). Furthermore, *n*E predicted MEP variance significantly (ROI_{HK}: 0.5 mA-tDCS: $R^2 = 0.40$, $p = 0.027$, r = 0.63, and 1.0 mA-tDCS: $R^2 = 0.44$, $p_{FDR} = 0.015$, r = 0.66; ROI_{TMS}: 0.5 mA-tDCS: $R^2 = 0.36$, $p_{FDR} = 0.034$, r = 0.60, and 2.0 mA-tDCS: $R^2 = 0.39$, $p_{FDR} = 0.042$, r = 0.62), Fig. 3A. However, none of the predictors explained the MEP variabilities of anodal tDCS at the late epoch, Fig. 3B. For the *cathodal group*, rCSF thickness only explained the MEP variance of 1.0 mA-tDCS (early epoch: $R^2 = 0.60$, $p_{FDR} < 0.001$, r = −0.77; late epoch: $R^2 = 0.40$, $p_{FDR} = 0.048$, r = −0.63). In addition, |E| and *n*E, both at ROI_{HK}, predicted MEP variabilities induced by tDCS with 1.0 mA (early epoch $R^2 = 0.54$, $p_{FDR} = 0.018$, r = 0.73; $R^2 = 0.45$, $p_{FDR} = 0.030$, r = 0.67; late epoch, only *n*E: $R^2 = 0.49$, $p_{FDR} = 0.027$, r = 0.70). For ROI_{TMS}, only |E| explained variabilities induced by tDCS with 1.0 mA (early epoch: $R^2 = 0.44$, $p_{FDR} = 0.030$, r = 0.66, late epoch: $R^2 = 0.48$, $p_{FDR} = 0.027$, r = 0.69), Fig. 4. For the complete statistical results, see supplementary material Tables 6 and 7, Fig. 6.

3.2. Association between anatomical factors, electrical fields and tDCS-induced CBF alterations

The results indicate that for the *anodal group*, at the early epoch, rCSF thickness significantly predicted CBF variabilities (1.0 mA-tDCS: $R^2 = 0.50$, $p_{FDR} = 0.014$, r = −0.73, and 2.0 mA-tDCS: $R^2 = 0.45$, $p_{FDR} = 0.028$, r = −0.67). In addition, |E| explained the CBF variance with significant predictive power (ROI_{HK}: 1.0 mA-tDCS: $R^2 = 0.59$, $p_{FDR} = 0.014$, r = 0.74, and 2.0 mA-tDCS: $R^2 = 0.44$, $p_{FDR} = 0.014$, r = 0.66), and a comparable result was obtained for *n*E (ROI_{HK}: 1.0 mA-tDCS: $R^2 = 0.48$, $p_{FDR} = 0.014$, r = 0.69, and 2.0 mA-tDCS: $R^2 = 0.40$, $p_{FDR} = 0.048$, r = 0.60), Fig. 5A1. However, none of the predictors explained the CBF variabilities at the late epoch, Fig. 5A2. For the *cathodal group*, none of the predictors explained the CBF variabilities at the early epoch, Fig. 5B1. However, for the late epoch, rCSF thickness, and rECD significantly predicted CBF variabilities (1.5 mA-tDCS: $R^2 = 0.61$, $p_{FDR} = 0.014$, r = −0.78; 2.0 mA-tDCS: $R^2 = 0.63$, $p_{FDR} = 0.021$, r = −0.79), respectively. In addition, |E| at ROI_{HK} explained the CBF variance with significant predictive power (1.5 mA-tDCS: $R^2 = 0.55$, $p_{FDR} = 0.014$, r = 0.74, 2.0 mA-tDCS $R^2 = 0.48$, $p_{FDR} = 0.043$, r = 0.69), and a similar result was obtained for *n*E at ROI_{HK} (1.5 mA-tDCS: $R^2 = 0.47$, $p_{FDR} = 0.021$, r = 0.69) Fig. 5B2. For the complete statistical results, see supplementary material Tables 8 and 9, Fig. 7.

4. Discussion

In the present study, we investigated the association between individual anatomical factors and tDCS-induced EF, and the

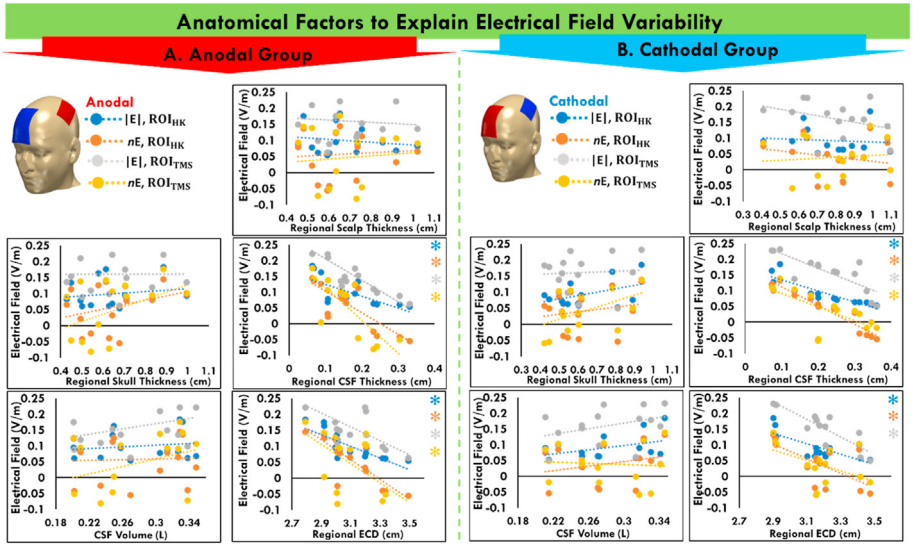

Fig. 2. Scatterplots of the association between Anatomical Factors and Electrical Fields. Anatomical factors, including *regional* scalp, skull and CSF thickness, CSF volume and *regional* electrode to cortex distance (rECD), and averaged EFs (magnitude (|E|) and normal components (nE)) were extracted from two ROIs (ROI_{HK} and ROI_{TMS}), for anodal and cathodal tDCS groups. The best-fitting regression lines are superimposed. Asterisks indicate significant results. Note that EFs are calculated for 1 mA tDCS, but due to the quasi-static assumption, estimated EFs are linearly scaled for other tDCS intensities.

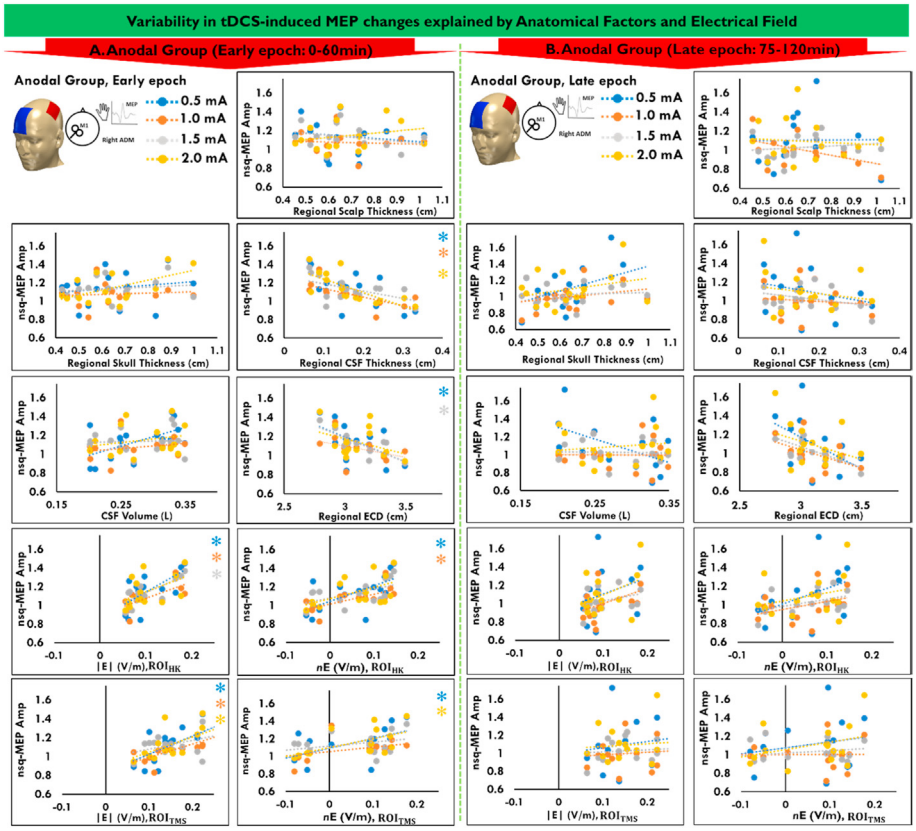

Fig. 3. Scatterplots of the association between Anatomical Factors, Electrical Fields, and anodal tDCS-induced MEP Alterations. The impact of anatomical factors including *regional* scalp, skull and CSF (rCSF) thickness, CSF volume and *regional* electrode to cortex distance (rECD), and averaged EFs (magnitude (|E|) and normal components (nE)) extracted from two ROIs (ROI_{HK} and ROI_{TMS}), for the anodal tDCS group, on MEP amplitude alterations (**A**: the early epoch (0–60min) and **B**: late epochs (75–120min) after stimulation) is depicted. The best-fitting regression lines are superimposed. Asterisks indicate significant results. nsq: square root of normalized (to baseline) measures. Note that EFs are calculated for 1 mA tDCS, but, due to the quasi-static assumption, the estimated EFs scale linearly for other tDCS intensities.

respective physiological outcomes of tDCS on MEP and CBF, at the level of the individual. In general, the results indicate that higher EF values were associated with lower rCSF thickness and rECD. In addition, rCSF thickness and rECD, as well as EFs, predicted physiological effects of stimulation, where tDCS altered MEP or CBF in comparison with respective baseline and/or sham values. This suggests that for prediction of local neurophysiological tDCS effects, the identified anatomical factors and EF, which are related to each other, are suited parameters.

The results are in accordance with previous findings, in which rCSF thickness and also rECD were suggested as key factors of EF simulations, and negatively correlated with individual EFs [7,19]. Furthermore, the results are in accordance with those of another study showing a positive correlation between EF parameters and physiological outcomes of the intervention [22]. An opposing finding was however reported for 1 mA anodal tDCS-induced EFs and individual MEP amplitude alterations in another study, where no significant MEP modulations were observed for the active condition vs. sham [21]. The missing overall effect of tDCS in that study is however in line with our findings in which the significant association between the predictors and the neurophysiological effects were obtained only for epochs with observed physiological responses.

4.1. Neurophysiological effects of tDCS on MEP and CBF

For the group-level **effects of tDCS on MEP,** previous studies suggest that regional after-effects of tDCS are based on modulation of synaptic efficacy, which is controlled by NMDA receptors and calcium influx [44]. Here, the stable facilitatory effects of all tested anodal tDCS intensities on MEP amplitudes indicate that all of these protocols most likely induced calcium influx within the range of excitatory effects. Respective studies showed furthermore dosage-dependent non-linear effects mainly for cathodal tDCS, which can also be explained by calcium dynamics [45–47]. The lack of plasticity induction accomplished by 0.5 mA cathodal tDCS can be explained by an insufficient alteration of calcium influx, while stimulation with 1 mA would alter calcium to an amount which is sufficient to induce long-term depression (LTD)-like plasticity. Higher stimulation intensities (1.5 mA and 2 mA) would then increase calcium concentration to a level above the LTD-inducing zone (so-called 'no man's land') [48]. **For the group-level effects of tDCS on CBF,** it has been shown that NMDA receptor activity modulates cerebral blood flow through neurovascular coupling, resulting in arterial vasodilation [49]. However, in difference to the MEP results, here a stimulation intensity-dependent linear effect on CBF was observed, similar to previous findings [50]. In addition to the aforementioned mechanisms, this might be caused by direct effects of tDCS on vessel dilation, but also effects of tDCS on astrocytic activity, which play a role in the regulation of blood flow [51].

With this in mind, the question emerges if these mechanisms could explain also the observed **inter-individual variability of the tDCS-induced neurophysiological effects.** The answer to this question is not trivial, due to the complexity of individual factors proposed to affect tDCS outcomes (see above). However, a

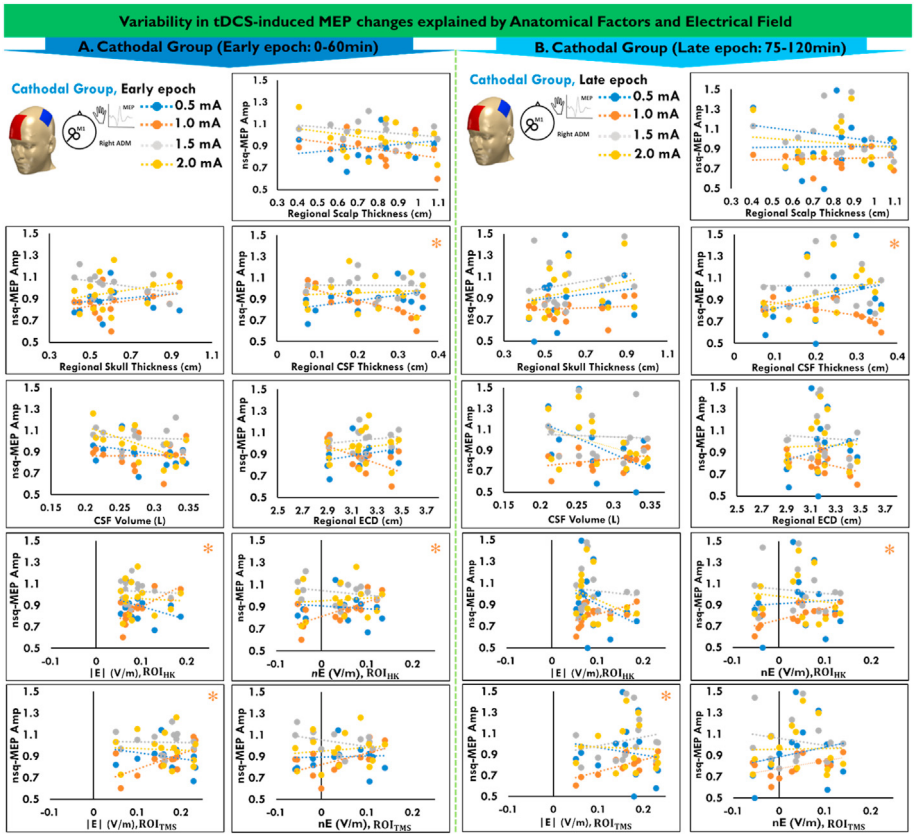

Fig. 4. Scatterplots of the association between Anatomical Factors, Electrical Fields, and cathodal tDCS-induced MEP Alterations. The impact of anatomical factors including *regional* scalp, skull and CSF (rCSF) thickness, CSF volume and *regional* electrode to cortex distance (rECD), and averaged EFs (magnitude (|E|) and normal components (nE)) extracted from two ROIs (ROI_{HK} and ROI_{TMS}), for the cathodal tDCS group on MEP amplitude alterations (**A**: the early epoch (0–60min) and **B**: late epoch (75–120min) after stimulation) is depicted. The best-fitting regression lines are superimposed. Asterisks indicate significant results. nsq: square root of normalized (to baseline) measures. Note that EFs are calculated for 1 mA tDCS, but, due to the quasi-static assumption, the estimated EFs scale linearly for other tDCS intensities.

moderate to high positive correlation between repeated neurophysiological measures ('tDCS conditions'; see supplementary materials Table 2), together with the significant effect observed for the respective tDCS protocols, and the significant explanatory power of the tested physical factors, suggest that the tested physical measures are well suited for predictions of tDCS-induced physiological effects. In what follows, we discuss the main findings in more detail.

4.2. Association between Anatomical Factors and Electrical Fields

The high inter-individual anatomical variability of respective tissues has been shown to strongly contribute to tDCS-induced EF variability across subjects [4]. Despite the complex interplay between tissue compartments, we found that a major part of the variance of the regional EFs can be explained by individual rCSF thickness and rECD. With respect to the relevance of rCSF, a thicker layer of CSF results in weaker EF at the level of the cortical target areas [7,19]. Indeed, the significant role of rCSF thickness might be due to the considerably larger electrical conductivity of CSF compared to other brain tissues, resulting in a preferential pathway for the injected currents. In the same vein, for rECD, this finding is supported by reports showing that resting motor threshold, which is positively correlated with scalp-to-cortex distance [52], correlates negatively with tDCS-induced EF magnitude [20]. It can be thus assumed that a larger rECD results in lower current densities, and EF induced by tDCS over the targeted area. The lack of predictive power of the other anatomical factors might be related to their limited volumes, and heterogeneous electrical conductivities.

4.3. Association between anatomical factors, electrical fields and tDCS-induced MEP and CBF alterations

For the **anodal tDCS-generated after-effects,** the positive correlation between individual rCSF thickness, rECD, and EFs fits nicely with the prior findings, indicating stimulation intensity-dependent increased efficacy of anodal tDCS to enhance MEP amplitudes, and CBF changes, as far as these can be dedicated to neuronal effects (all tested tDCS intensities for MEP; tDCS with 1 mA and 2 mA intensity for CBF). In contrast, our results showed a more limited predictive power of rCSF thickness, rECD, and EF for explaining intensity-dependent **cathodal tDCS after-effects** on MEP alterations, as the clearest effects with respect to the association of EF, and MEP size were seen for the stimulation intensity of 1.0 mA. This might be caused to some degree by the non-linear physiological effects of motor cortex cathodal tDCS within the tested dosage range (as already shown in other studies [53,54]; see above for details). For cathodal tDCS-induced after-effects on CBF, a similar association was observed for higher intensities (1.5 mA and 2 mA), but only for late epochs. The missing predictive power of the explanatory variables for the early epoch in these conditions can be explained by non-homogeneous effects of cathodal tDCS on neural excitability, and vessels, as well as different temporal dynamics of the respective contributions (as explained above). At present, these

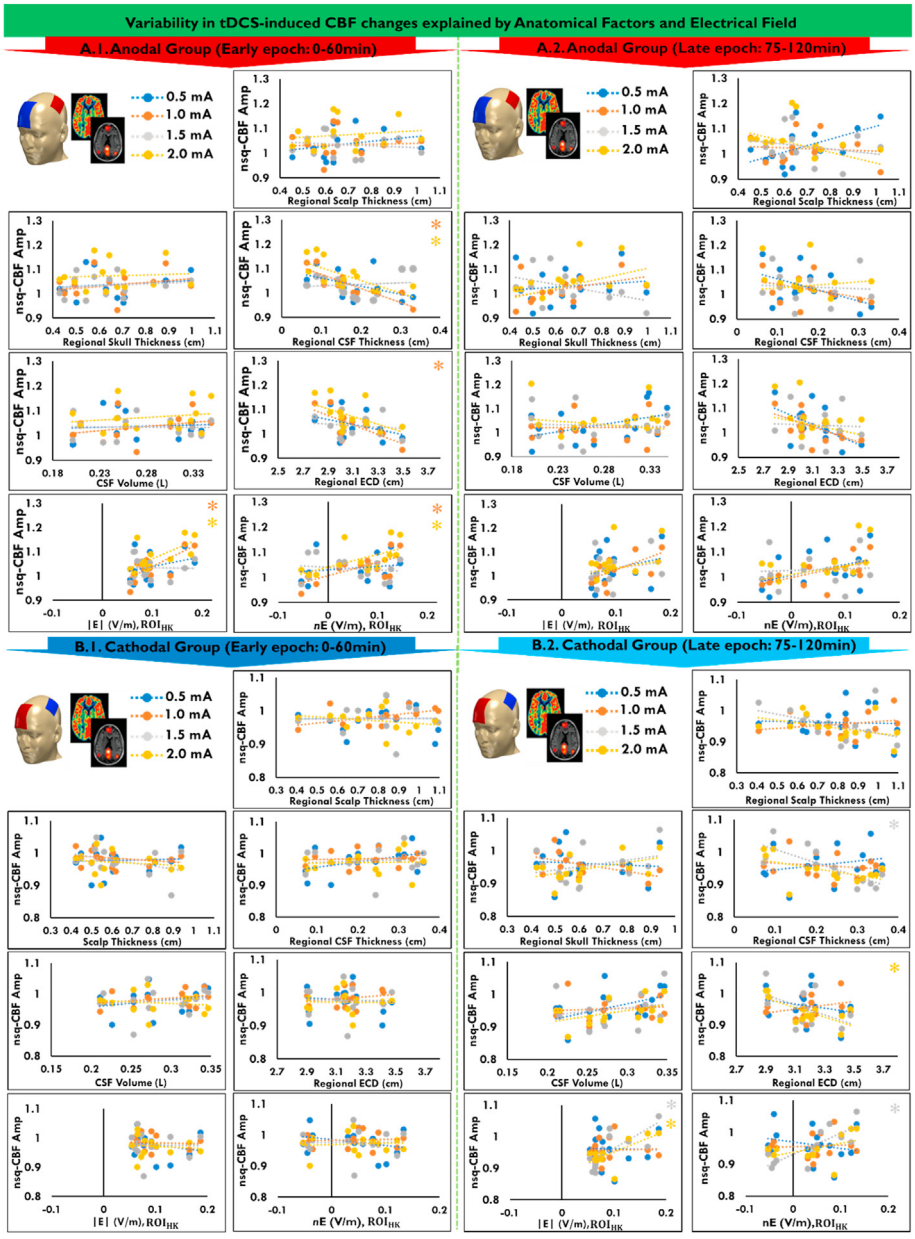

Fig. 5. Anatomical factors and electrical field values to explain tDCS-induced CBF alterations. The impact of anatomical factors including *regional* scalp, skull and CSF (rCSF) thickness, CSF volume and *regional* electrode to cortex distance (rECD), and averaged EFs (magnitude |E|, and normal components *n*E) at ROI_{HK} were explored with respect to their predictive power for CBF variabilities of four active tDCS conditions (0.5 mA, 1.0 mA, 1.5 mA and 2.0 mA) for early (0–60min) and late (75–120min) epochs after stimulation, for the anodal tDCS (A1,2), and cathodal (B1,2) groups. The best-fitting regression lines are superimposed. Asterisks indicate significant results. nsq: square root of normalized (to baseline) measures. Note that EFs are calculated for 1 mA tDCS, but, due to the quasi-static assumption, the estimated EFs scale linearly for other tDCS intensities.

explanations are speculative and should be explored in future studies directly.

Limitations and future directions

This study should be interpreted within the context of some limitations. At the neurophysiological level, due to the exploratory character of our study, further confirmatory research, ideally with larger sample size, is needed. In addition, while the model used in this study showed relatively good predictions of tDCS-induced physiological effects, further research is required to test if individual model-based adjustment of tDCS parameters will reduce inter-individual variability of the stimulation effects [55]. Furthermore, recent studies have suggested that several other individual anatomical factors (e.g. absolute head volume and relative volume of skin, skull and CSF [56], as well as anatomical details of the skin [57]) are relevant for the tDCS-induced EF. Conceptually, EF, and especially the normal component of EF, which takes into account directional differences of EF due to stimulation polarity, should be better suited to predict physiological tDCS effects than single anatomical factors, because it is based on the contribution of all potentially relevant anatomical factors. However, the results of the present study suggest that in case of non-availability of modeling approaches, anatomical factors such as electrode-to- cortex distance are suited as reasonable proxies. Moreover, beyond the physical factors, other confounding factors (as explained above)

might also contribute to inter-individual variability of tDCS outcome, and should be considered in future studies. Also, transferability of the results from the motor cortex to other brain regions [58,59], other ages [13,60,61], other stimulation parameters [62–64], and clinical populations [65–67] should not be taken for granted, but require experimental proof. Also, our results were mainly based on regional effects of tDCS, future studies might broaden their scope to network effects of locally induced interventions.

At the computational level, the modeling pipeline might be improved by including other relevant tissues, such as muscles and fat [68], considering individual head tissue electrical conductivities, and anisotropic conductivity [69–72]. In addition, recent studies highlighted the sensitivity of EF simulation to differences of modeling pipelines (e.g. segmentation of anatomy which results in errors [34]) [73], but also implemented head tissue electrical conductivity [8,74]. The structural MRI resolution of the present study (1 mm^3) is in accordance with the typical ones used in modeling studies [75], and the assumed electrical tissue conductivity values used in this study are comparable with the ones which have been used in previous studies, and it has been shown in these studies that EFs calculated on this basis correlate well with in-vivo intracranial EF recordings [18]. We thus assume that the MRI resolution in this study, together with the used tissue electrical conductivities are appropriate. In addition, we made efforts to reduce segmentation errors, e.g. by post-processing the segmented images to improve compatibility with the original MR images. It should however be noted that there is not yet a general consensus on the optimal head tissues conductivity values for tDCS application. As a result, different conductivity values are used in different studies and there is an on-going debate about their accuracy. While investigating these issues is out of the scope of this study, a sensitivity analyses of the impact of those factors on the qauntification of EFs might improve the impact of findings [8]. Furthermore, to improve and document the consistency of electrode placement across sessions further, neuronavigation might have been advantageous. However, since baseline measures (MEP, CBF, and TMS intensities) in the current study did not differ between sessions, we assume that electrode positions, which were determined for each session physiologically via mapping the ADM hotspot via TMS, did not differ relevantly between sessions [76]. Finally, MRI studies have shown that CSF thickness changes when a subject moves from a prone to a supine position [77,78]. This has been shown to affect EF simulations of tDCS effects at about 10% [79]. This is relevant, as tDCS is applied usually when the subject is in an upright position, whereas MR images are typically acquired with the subject lying in a supine position. Thus the exact extent to which the individual MR-derived EF simulations represent the EF distribution in physiological measures performed in sitting participants is debatable and should be investigated in future studies.

Conclusions

This study shows that individual anatomical factors (including regional CSF thickness (rCSF) and regional electrode to cortex distance (rECD)), significantly explain inter-individual EF variabilities. In addition, rCSF thickness, and rECD were negatively correlated, whereas EFs were positively correlated with tDCS-induced physiological changes. It general, our study demonstrates the usefulness of computational modeling, similar to the one used in this study, for the prediction of EF, and physiological effects induced by tDCS. However, considering other relevant head tissues, anisotropic conductivity, as well as individual electrical conductivity, and neuronal models might improve modeling accuracy and potentially the predictive power for the neurophysiolocal effects of tDCS. In addition, the transferability of these results to other cortical areas, age, and patient populations should be considered in future studies. This study provides further insights into the dependency of neuromodulatory effects of tDCS from individual anatomy, and the usefulness of electrical field simulations, and therefore delivers crucial information for future applications.

Funding

This work was supported by a research grant from the German Federal Ministry of Education and Research (BMBF) (GCBS grant 01EE1501, TRAINSTIM grant 01GQ1424E).

CRediT authorship contribution statement

Mohsen Mosayebi-Samani: Conceptualization, Data curation, Formal analysis, Investigation, Writing - original draft, Writing - review & editing. **Asif Jamil:** Neurophysiological acquisition and analysis, review & editing. **Ricardo Salvador:** Methodology, Validation, Writing - review & editing. **Giulio Ruffini:** Methodology, Validation, Writing - review & editing. **Jens Haueisen:** Conceptualization, Supervision, Methodology, Validation, Writing - review & editing. **Michael A. Nitsche:** Conceptualization, Funding acquisition, Supervision, Methodology, Validation, Writing - review & editing.

Declaration of competing interest

MA Nitsche is member of Advisory Board of Neuroelectrics and NeuroDevice. Giulio Ruffini is a shareholder and works for Neuroelectrics. Ricardo Salvador works for Neuroelectrics. None of the remaining authors have potential conflicts of interest to be disclosed.

Appendix A. Supplementary data

Supplementary data related to this article can be found at https://doi.org/10.1016/j.brs.2021.01.016.

References

[1] Yavari F, Jamil A, Mosayebi Samani M, Vidor LP, Nitsche MA. Basic and functional effects of transcranial Electrical Stimulation (tES)—an introduction. Neurosci Biobehav Rev 2018;85:81–92.
[2] Lefaucheur JP, Antal A, Ayache SS, Benninger DH, Brunelin J, Cogiamanian F, et al. Evidence-based guidelines on the therapeutic use of transcranial direct current stimulation (tDCS). Clin Neurophysiol : official journal of the International Federation of Clinical Neurophysiology 2017;128(1):56–92.
[3] Huang YZ, Lu MK, Antal A, Classen J, Nitsche M, Ziemann U, et al. Plasticity induced by non-invasive transcranial brain stimulation: a position paper. Clin Neurophysiol : official journal of the International Federation of Clinical Neurophysiology 2017;128(11):2318–29.
[4] Li LM, Uehara K, Hanakawa T. The contribution of interindividual factors to variability of response in transcranial direct current stimulation studies. Front Cell Neurosci 2015;9:181.
[5] Wiethoff S, Hamada M, Rothwell JC. Variability in response to transcranial direct current stimulation of the motor cortex. Brain stimulation 2014;7(3):468–75.
[6] Strube W, Bunse T, Nitsche MA, Nikolaeva A, Palm U, Padberg F, et al. Bidirectional variability in motor cortex excitability modulation following 1 mA transcranial direct current stimulation in healthy participants. Physiological reports 2016;4(15). e12884.
[7] Laakso I, Tanaka S, Koyama S, De Santis V, Hirata A. Inter-subject variability in electric fields of motor cortical tDCS. Brain stimulation 2015;8(5):906–13.
[8] Saturnino GB, Thielscher A, Madsen KH, Knösche TR, Weise K. A principled approach to conductivity uncertainty analysis in electric field calculations. Neuroimage 2019;188:821–34.
[9] Shahid SS, Bikson M, Salman H, Wen P, Ahfock T. The value and cost of complexity in predictive modelling: role of tissue anisotropic conductivity and fibre tracts in neuromodulation. J Neural Eng 2014;11(3). 036002.

[10] Rahman A, Reato D, Arlotti M, Gasca F, Datta A, Parra LC, et al. Cellular effects of acute direct current stimulation: somatic and synaptic terminal effects. J Physiol 2013;591(10):2563–78.
[11] Wiegand A, Nieratschker V, Plewnia C. Genetic modulation of transcranial direct current stimulation effects on cognition. Front Hum Neurosci 2016;10:651.
[12] Kuo M-F, Paulus W, Nitsche MA. Sex differences in cortical neuroplasticity in humans. Neuroreport 2006;17(16):1703–7.
[13] Ghasemian-Shirvan E, Farnad L, Mosayebi-Samani M, Verstraelen S, Meesen RLJ, Kuo M-F, et al. Age-related differences of motor cortex plasticity in adults: a transcranial direct current stimulation study. Brain stimulation 2020;13(6):1588–99.
[14] Fresnoza S, Paulus W, Nitsche MA, Kuo M-F. Nonlinear dose-dependent impact of D1 receptor activation on motor cortex plasticity in humans. J Neurosci 2014;34(7):2744–53.
[15] Tseng P, Hsu TY, Chang CF, Tzeng OJ, Hung DL, Muggleton NG, et al. Unleashing potential: transcranial direct current stimulation over the right posterior parietal cortex improves change detection in low-performing individuals. J Neurosci : the official journal of the Society for Neuroscience 2012;32(31):10554–61.
[16] Furuya S, Klaus M, Nitsche MA, Paulus W, Altenmüller E. Ceiling effects prevent further improvement of transcranial stimulation in skilled musicians. J Neurosci 2014;34(41):13834–9.
[17] Opitz A, Falchier A, Yan CG, Yeagle EM, Linn GS, Megevand P, et al. Spatiotemporal structure of intracranial electric fields induced by transcranial electric stimulation in humans and nonhuman primates. Sci Rep 2016;6:31236.
[18] Huang Y, Liu AA, Lafon B, Friedman D, Dayan M, Wang X, et al. Measurements and models of electric fields in the in vivo human brain during transcranial electric stimulation, vol. 6; 2017.
[19] Opitz A, Paulus W, Will S, Antunes A, Thielscher A. Determinants of the electric field during transcranial direct current stimulation. Neuroimage 2015;109:140–50.
[20] Mikkonen M, Laakso I, Sumiya M, Koyama S, Hirata A, Tanaka S. TMS motor thresholds correlate with TDCS electric field strengths in hand motor area. Front Neurosci 2018;12(426).
[21] Laakso I, Mikkonen M, Koyama S, Hirata A, Tanaka S. Can electric fields explain inter-individual variability in transcranial direct current stimulation of the motor cortex? Sci Rep 2019;9(1):626.
[22] Antonenko D, Thielscher A, Saturnino GB, Aydin S, Ittermann B, Grittner U, et al. Towards precise brain stimulation: is electric field simulation related to neuromodulation? Brain stimulation. Brain stimulation; 2019;12(5):1159-68.
[23] Kim JH, Kim DW, Chang WH, Kim YH, Kim K, Im CH. Inconsistent outcomes of transcranial direct current stimulation may originate from anatomical differences among individuals: electric field simulation using individual MRI data. Neurosci Lett 2014;564:6–10.
[24] Kasten FH, Duecker K, Maack MC, Meiser A, Herrmann CS. Integrating electric field modeling and neuroimaging to explain inter-individual variability of tACS effects. Nat Commun 2019;10(1):5427.
[25] Bestmann S, Krakauer JW. The uses and interpretations of the motor-evoked potential for understanding behaviour. Exp Brain Res 2015;233(3):679–89.
[26] Salvador R, Silva S, Basser PJ, Miranda PC. Determining which mechanisms lead to activation in the motor cortex: a modeling study of transcranial magnetic stimulation using realistic stimulus waveforms and sulcal geometry. Clin Neurophysiol 2011;122(4):748–58.
[27] Weise K, Numssen O, Thielscher A, Hartwigsen G, Knösche TR. A novel approach to localize cortical TMS effects. Neuroimage 2020;209. 116486.
[28] Jamil A, Batsikadze G, Kuo HI, Labruna L, Hasan A, Paulus W, et al. Systematic evaluation of the impact of stimulation intensity on neuroplastic after-effects induced by transcranial direct current stimulation. J Physiol 2017;595(4):1273–88.
[29] Jamil A, Batsikadze G, Kuo HI, Meesen RL, Dechent P, Paulus W, et al. Current intensity-and polarity-specific online and aftereffects of transcranial direct current stimulation: an fMRI study. Human brain mapping. Human brain mapping; 2020; 41(6):1644-66.
[30] Oldfield RC. The assessment and analysis of handedness: the Edinburgh inventory. Neuropsychologia 1971;9(1):97–113.
[31] Bikson M, Grossman P, Thomas C, Zannou AL, Jiang J, Adnan T, et al. Safety of transcranial direct current stimulation: evidence based update 2016. Brain stimulation 2016;9(5):641–61.
[32] Rossi S, Hallett M, Rossini PM, Pascual-Leone A, Group SoTC. Safety, ethical considerations, and application guidelines for the use of transcranial magnetic stimulation in clinical practice and research. Clin Neurophysiol 2009;120(12):2008–39.
[33] McFadden JL, Borckardt JJ, George MS, Beam W. Reducing procedural pain and discomfort associated with transcranial direct current stimulation. Brain stimulation 2011;4(1):38–42.
[34] Huang Y, Dmochowski JP, Su Y, Datta A, Rorden C, Parra LC. Automated MRI segmentation for individualized modeling of current flow in the human head. J Neural Eng 2013;10(6). 066004.
[35] Datta A, Bansal V, Diaz J, Patel J, Reato D, Bikson M. Gyri-precise head model of transcranial direct current stimulation: improved spatial focality using a ring electrode versus conventional rectangular pad. Brain stimulation 2009;2(4):201–207. e1.
[36] Wagner T, Fregni F, Fecteau S, Grodzinsky A, Zahn M, Pascual-Leone A. Transcranial direct current stimulation: a computer-based human model study. Neuroimage 2007;35(3):1113–24.
[37] Miranda PC, Mekonnen A, Salvador R, Ruffini G. The electric field in the cortex during transcranial current stimulation. Neuroimage 2013;70:48–58.
[38] Deng ZD, Lisanby SH, Peterchev AV. Electric field depth-focality tradeoff in transcranial magnetic stimulation: simulation comparison of 50 coil designs. Brain stimulation 2013;6(1):1–13.
[39] Miranda PC, Correia L, Salvador R, Basser PJ. Tissue heterogeneity as a mechanism for localized neural stimulation by applied electric fields. Phys Med Biol 2007;52(18):5603–17.
[40] Wagner TA, Zahn M, Grodzinsky AJ, Pascual-Leone A. Three-dimensional head model simulation of transcranial magnetic stimulation. IEEE Trans Biomed Eng 2004;51(9):1586–98.
[41] McDonald JH. Handbook of biological statistics. MD: sparky house publishing Baltimore; 2009.
[42] Pimentel MA, Vilela P, Sousa I, Figueiredo P. Localization of the hand motor area by arterial spin labeling and blood oxygen level-dependent functional magnetic resonance imaging. Hum Brain Mapp 2013;34(1):96–108.
[43] Carbunaru R, Durand DM. Toroidal coil models for transcutaneous magnetic simulation of nerves. IEEE (Inst Electr Electron Eng) Trans Biomed Eng 2001;48(4):434–41.
[44] Stagg CJ, Nitsche MA. Physiological basis of transcranial direct current stimulation. Neuroscientist 2011;17(1):37–53.
[45] Mosayebi-Samani M, Melo L, Agboada D, Nitsche MA, Kuo MF. Ca2+ channel dynamics explain the nonlinear neuroplasticity induction by cathodal transcranial direct current stimulation over the primary motor cortex. work submitted for publication; 2020;38. p. 63–72.
[46] Hassanzahraee M, Nitsche MA, Zoghi M, Jaberzadeh S. Determination of anodal tDCS duration threshold for reversal of corticospinal excitability: an investigation for induction of counter-regulatory mechanisms. Brain stimulation 2020;13(3):832–9.
[47] Nitsche M, Fricke K, Henschke U, Schlitterlau A, Liebetanz D, Lang N, et al. Pharmacological modulation of cortical excitability shifts induced by transcranial direct current stimulation in humans. J Physiol 2003;553(1):293–301.
[48] Lisman JE. Three Ca2+ levels affect plasticity differently: the LTP zone, the LTD zone and no man's land. J Physiol 2001;532(2):285.
[49] Attwell D, Buchan AM, Charpak S, Lauritzen M, MacVicar BA, Newman EA. Glial and neuronal control of brain blood flow. Nature 2010;468(7321):232–43.
[50] Zheng X, Alsop DC, Schlaug G. Effects of transcranial direct current stimulation (tDCS) on human regional cerebral blood flow. Neuroimage 2011;58(1):26–33.
[51] MacVicar BA, Newman EA. Astrocyte regulation of blood flow in the brain. Cold Spring Harbor perspectives in biology 2015;7(5).
[52] Kozel FA, Nahas Z, deBrux C, Molloy M, Lorberbaum JP, Bohning D, et al. How coil-cortex distance relates to age, motor threshold, and antidepressant response to repetitive transcranial magnetic stimulation. J Neuropsychiatry Clin Neurosci 2000;12(3):376–84.
[53] Mosayebi Samani M, Agboada D, Jamil A, Kuo M-F, Nitsche MA. Titrating the neuroplastic effects of cathodal transcranial direct current stimulation (tDCS) over the primary motor cortex. Cortex 2019;119:350–61.
[54] Batsikadze G, Moliadze V, Paulus W, Kuo MF, Nitsche M. Partially non-linear stimulation intensity-dependent effects of direct current stimulation on motor cortex excitability in humans. J Physiol 2013;591(7):1987–2000.
[55] Evans C, Bachmann C, Lee JSA, Gregoriou E, Ward N, Bestmann S. Dose-controlled tDCS reduces electric field intensity variability at a cortical target site. Brain stimulation 2020;13(1):125–36.
[56] Antonenko D, Grittner U, Saturnino G, Nierhaus T, Thielscher A, Flöel A. Inter-individual and age-dependent variability in simulated electric fields induced by conventional transcranial electrical stimulation. Neuroimage 2021;224.117413.
[57] Khadka N, Bikson M. Role of skin tissue layers and ultra-structure in transcutaneous electrical stimulation including tDCS. Phys Med Biol 2020;65(22).225018.
[58] Antal A, Kincses TZ, Nitsche MA, Bartfai O, Paulus W. Excitability changes induced in the human primary visual cortex by transcranial direct current stimulation: direct electrophysiological evidence. Investig Ophthalmol Vis Sci 2004;45(2):702–7.
[59] Hill AT, Rogasch NC, Fitzgerald PB, Hoy KE. Effects of prefrontal bipolar and high-definition transcranial direct current stimulation on cortical reactivity and working memory in healthy adults. Neuroimage 2017;152:142–57.
[60] Ciechanski P, Carlson HL, Yu SS, Kirton A. Modeling transcranial direct-current stimulation-induced electric fields in children and adults. Front Hum Neurosci 2018;12(268).
[61] Indahlastari A, Albizu A, O'Shea A, Forbes MA, Nissim NR, Kraft JN, et al. Modeling transcranial electrical stimulation in the aging brain. Brain stimulation 2020;13(3):664–74.
[62] Agboada D, Mosayebi Samani M, Jamil A, Kuo M-F, Nitsche MA. Expanding the parameter space of anodal transcranial direct current stimulation of the primary motor cortex. Sci Rep 2019;9(1). 18185.
[63] Agboada D, Mosayebi-Samani M, Kuo M-F, Nitsche MA. Induction of long-term potentiation-like plasticity in the primary motor cortex with repeated anodal transcranial direct current stimulation – better effects with intensified protocols? Brain stimulation 2020;13(4):987–97.

[64] Mosayebi Samani M, Agboada D, Kuo MF, Nitsche MA. Probing the relevance of repeated cathodal transcranial direct current stimulation over the primary motor cortex for prolongation of after-effects. J Physiol 2020;598(4):805–16.
[65] Hoy KE, Arnold SL, Emonson MR, Daskalakis ZJ, Fitzgerald PB. An investigation into the effects of tDCS dose on cognitive performance over time in patients with schizophrenia. Schizophr Res 2014;155(1–3):96–100.
[66] Boggio PS, Ferrucci R, Rigonatti SP, Covre P, Nitsche M, Pascual-Leone A, et al. Effects of transcranial direct current stimulation on working memory in patients with Parkinson's disease. J Neurol Sci 2006;249(1):31–8.
[67] Datta A, Baker JM, Bikson M, Fridriksson J. Individualized model predicts brain current flow during transcranial direct-current stimulation treatment in responsive stroke patient. Brain stimulation 2011;4(3):169–74.
[68] Truong DQ, Magerowski G, Blackburn GL, Bikson M, Alonso-Alonso M. Computational modeling of transcranial direct current stimulation (tDCS) in obesity: impact of head fat and dose guidelines. Neuroimage: Clinical 2013;2:759–66.
[69] McCann H, Pisano G, Beltrachini L. Variation in reported human head tissue electrical conductivity values. Brain Topogr 2019;32(5):825–58.
[70] Rampersad SM, Janssen AM, Lucka F, Aydin U, Lanfer B, Lew S, et al. Simulating transcranial direct current stimulation with a detailed anisotropic human head model. IEEE Trans Neural Syst Rehabil Eng : a publication of the IEEE Engineering in Medicine and Biology Society 2014;22(3):441–52.
[71] Wagner S, Rampersad SM, Aydin U, Vorwerk J, Oostendorp TF, Neuling T, et al. Investigation of tDCS volume conduction effects in a highly realistic head model. J Neural Eng 2014;11(1). 016002.
[72] Mosayebi Samani M, Firoozabadi SM, Ekhtiari H. Consideration of individual brain geometry and anisotropy on the effect of tDCS. Iranian Journal of Medical Physics 2017;14(4):203–18.
[73] Puonti O, Saturnino GB, Madsen KH, Thielscher A. Value and limitations of intracranial recordings for validating electric field modeling for transcranial brain stimulation. Neuroimage 2020;208. 116431.
[74] McCann H, Pisano G, Beltrachini L. Variation in reported human head tissue electrical conductivity values. Brain Topogr. 2019;32(5):825–58.
[75] Windhoff M, Opitz A, Thielscher A. Electric field calculations in brain stimulation based on finite elements: an optimized processing pipeline for the generation and usage of accurate individual head models. Hum Brain Mapp 2013;34(4):923–35.
[76] Woods AJ, Antal A, Bikson M, Boggio PS, Brunoni AR, Celnik P, et al. A technical guide to tDCS, and related non-invasive brain stimulation tools. Clin Neurophysiol 2016;127(2):1031–48.
[77] Wallois F, Mahmoudzadeh M, Patil A, Grebe R. Usefulness of simultaneous EEG–NIRS recording in language studies. Brain Lang 2012;121(2):110–23.
[78] Rice JK, Rorden C, Little JS, Parra LC. Subject position affects EEG magnitudes. Neuroimage 2013;64:476–84.
[79] Mikkonen M, Laakso I. Effects of posture on electric fields of non-invasive brain stimulation. Phys Med Biol 2019;64(6). 065019.